Neural Accumulator Models of Decision Making in Eye Movements

Vassilis Cutsuridis

Abstract Humans and animals are constantly facing the problem of having to choose from a variety of possible actions as they interact with the environment. Both external and internal cues have to be used to guide their selection of a single action from many possible alternatives. Which action to choose in a given context may have important biological consequences to their survival. Decision making is regarded as an accumulation process of evidence about the state of the world and the utility of possible outcomes. Two well established neural accumulator models of decision making are presented to model the neural basis of decision making in behavioural paradigms such as the antisaccade task.

Keywords Superior colliculus · Antisaccade task · Decision making · Accumulator model · Eye movement

1 Introduction

Decision making is the process of selecting from sets of options based on current evidence about the state of the world and estimates of the value of different outcomes [1]. Decision making has been a topic of intense study by multiple disciplines such as economics, sociology, statistics, computer science, artificial intelligence, ethology, cognitive and behavioural neuroscience. Economists often investigate how decisions are formulated in the presence of uncertainty, whereas ethologists approach the problem of decision making in the context of foraging Psychologists frequently investigate a behavioural choice using a concurrent schedule of reinforcement. Sociologists investigate how the decision making processes of an individual are influenced by the decisions of others in the same group [11], whereas artificial

V. Cutsuridis (✉)
Department of Computing Science and Mathematics, University of Stirling, Stirling FK9 4LA, U.K.
e-mail: vcu@cs.stir.ac.uk

A. Hussain et al. (eds.), *Brain Inspired Cognitive Systems 2008*, Advances in Experimental Medicine and Biology 657, DOI 10.1007/978-0-387-79100-5_4,

intelligence (AI) and computer science analyze how an optimal decision-making strategy can be learned through experience [12].

In recent years, cognitive and behavioural neuroscientists have begun to investigate the neural basis of decision making using various behavioural paradigms. The behavioural paradigm often used is saccadic eye movements (i.e. rapid eye movements to bring the saccadic goal onto the fovea). Saccadic eye movements are important in understanding the neural basis of decision making, because (1) making a saccade, among a set of potential visual targets, one must be selected as the next end-point of a saccade and (2) initiating a saccade, the decision must be made to release the system from its previous state of fixation. The slowness, variability of response times (RT) and percentage of erroneous responses are some of the understudy variables in these behavioural paradigms.

In this paper, two neural accumulator models [2–7] of visually guided eye movements in the absence of distractors at various levels of abstraction (molecular, single neuron, population of neurons, multiple brain areas and behaviour) are summarized to provide functional roles to the neural substrates involved in preparation and execution of the saccadic eye movements and explain which neural mechanisms are responsible of the response variability and error rate in a well established oculomotor task (i.e. antisaccade task).

2 Brain Anatomy and Physiology of Saccade Eye Movements

Several brain areas are involved in the control of saccadic eye movements [13]. Visual information from the external world enters the brain from the eyes through two distinct anatomical pathways: (1) From the retino-geniculo-cortical pathway to the primary visual cortex and (2) from the retinotectal pathway to the superficial layers of the SC. Visual information is subsequently processed through several extrastriate visual areas before it arrives in the lateral intraprietal area (LIP) in the posterior parietal cortex. LIP is at the interface between sensory and motor processing. The LIP in turn projects to both the intermediate layers of the superior colliculus (SC) and the frontal cortical oculomotor areas including the frontal eye fields (FEF), the supplementary eye fields (SEF) and the dorsolateral prefrontal cortex (DLFPC). The FEF has a crucial role in executing voluntary saccades, whereas the SEF is important for internally guided decision-making and sequencing of saccades [14]. The DLPFC is involved in executive function, spatial working memory and suppressing automatic, reflexive responses [15]. All these frontal regions project then to the SC, which is a vital node in the premotor circuit where cortical and subcortical signals converge and are integrated.

Furthermore, the FEF, SEF and SC project directly to the reticular formation to provide the necessary input to the saccadic premotor circuit that a saccade is initiated or suppressed. Frontal and posterior cortical oculomotor areas also project indirectly to SC through the direct and indirect pathways of the basal ganglia. Cortical inputs to the direct pathway lead to disinhibition of the SC and thalamus, whereas cortical inputs to the indirect pathway lead to the inhibition of both SC and thalamus.

3 Empirical Signatures

A behavioural paradigm often used to investigate decision processes is the antisaccade task [10]. The antisaccade task is a choice reaction time task in which subjects perform eye movements in the opposite direction from the location of a peripheral stimulus [10]. Recently, a large epidemiological study was conducted [8, 9] testing the performance of a large population of young male subjects in the antisaccade oculomotor task. A population of 2075 conscripts performed 90 trials of the antisaccade task as fast as possible without any accuracy constraints (see Fig. 1). Each subject was seated in front of computer monitor and he/she was asked to fixate to a stimulus in the centre of the screen. After a variable period of 1–2 s, the central stimulus was extinguished and immediately after another stimulus appeared randomly at one of nine distances (2–10° at 1° intervals) either to left or to the right of the central fixation stimulus. The subjects were instructed to make an eye movement to the opposite direction from that of the peripheral stimulus as quickly as possible. The following indices of performance were measured:

- Percentage of errors
- Mean latency of the first eye movement regardless of whether this was an error prosaccade or a correct antisaccade eye movement
- Standard deviation of the latency of the first eye movement
- Mean latency of correct antisaccades
- Standard deviation of the latency of the correct antisaccades
- Mean latency of error prosaccades
- Standard deviation of the latency of the error prosaccades
- Mean latency of corrections
- Standard deviation of the latency of corrections

Saccade reaction time was defined as the time taken from the first appearance of the peripheral stimulus ‘till the first detectable eye movement. Trials with reaction times <80 ms were excluded as anticipations and trials with reaction times >600 ms were excluded as no response trials. Only three eye movement behaviours were observed: (1) the subject made the correct antisaccade, (2) the subject made the error

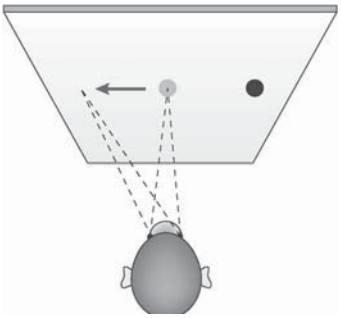

Fig. 1 Experimental setup of the antisaccade task (reproduced with permission from [14], Fig. 1,p. 221, Copyright © Nature publishing company)

prosaccade (very rare), and (3) the subject made an error prosaccade followed by a correct antisaccade. *At no time was ever observed a subject to make a correct antisaccade followed by an error prosaccade in the same trial.* A unimodal distribution of correct antisaccades and erroneous prosaccades were observed. The mean latency and standard deviation of the correct antisaccade from all subjects, respectively, were 270 ± 39ms and 56 ± 19ms. The mean latency and standard deviation of the error prosaccades from all subjects, respectively, were 208 ± 38ms and 46 ± 27ms. Finally, a 23% ± 17% of erroneous prosaccades of all subjects were reported.

These results raised some very important questions: (1) Why are the mean latencies of the correct antisaccades and error prosaccades so variable between trials in each subject and across all subjects? (2) Why the error rate is only 23%? Why not 50%? (3) What stops the error prosaccade from been expressed after the correct antisaccade has been released first? (4) Which are the neural mechanisms that justify these results?

These questions have been successfully addressed by the neural population accumulator model of the SC [2, 6, 7] summarized in the next section.

4 A Neural Population Accumulator Model of Decision Making Constrained by Antisaccade Data

The first model (see Fig. 2), which we will call the neural population accumulator model was a one-dimensional model of the intermediate layer of the superior colliculus (SC) [2,6,7]. The connectivity between neurons in the population was assumed to be on-centre off-surround. The internal state of each neuron i was given by

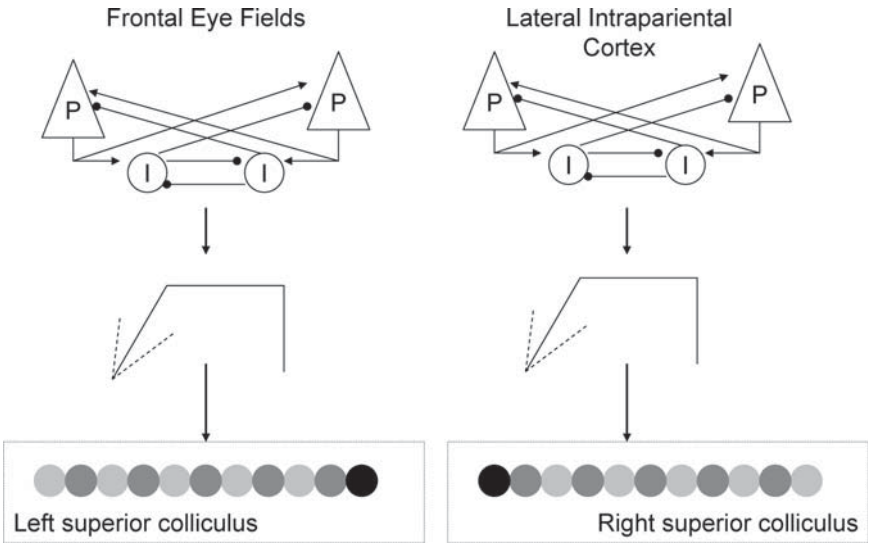

Fig. 2 Schematic diagram of the neural accumulator models

$$\tau \frac{dx_i(t)}{dt} = -x_i(t) + \sum_j w_{ij} A_j(t) + I_p(t) + I_r(t) - u_0 + I_n, \tag{1}$$

where I_n was the noise background input, u_0 was a global inhibition term, I_p and I_r were the two external inputs and τ was the integration constant. The average firing rate of each neuron was then given by

$$A_i(t) = \frac{1}{1 + \exp(-\beta u_i(t) + \theta)}, \tag{2}$$

where β was the sigmoid steepness and θ was the sigmoid offset. The interaction matrix between nodes was given by

$$w_{ij} = a \exp\left(\frac{-(j-i)^2}{2 \cdot \sigma_A^2}\right) - b \exp\left(\frac{-(j-i)^2}{2 \cdot \sigma_B^2}\right) - c, \tag{3}$$

where *a, b, c* were free parameters and σ_A, σ_B were spatial parameters. Three different types of SC neurons were modelled: fixation, buildup and burst neurons. Briefly, in the superior colliculus, fixation neurons discharge tonically when the subject is fixating and pause their activity when a saccade is initiated. On the other hand, buildup neurons discharge only when a saccade is initiated. Burst neurons discharge phasically and provide the final motor command to the brainstem neurons for the generation of an eye movement.

In the model, the two external inputs, which represented the FEF and LIP decision signals were modelled by

$$\begin{aligned}
&I = A \cdot |slope \cdot t|, && \text{if } t_{on} + t_{delay} \le t \le t_{off} + t_{delay} \text{ and } I < I_{\max} \\
&I = A \cdot I_{\max}, && \text{if } t_{on} + t_{delay} \le t \le t_{off} + t_{delay} \text{ and } I \ge I_{\max} \\
&I = 0, && \\
&A = \exp\left(\frac{-(j-i)^2}{2 \cdot \sigma_A^2}\right), &&
\end{aligned} \tag{4}$$

where t_{delay} was the conduction delay from the retina to LIP (70 ms) and FEF (120ms), I_{max} was the theoretical maximum SC neuronal activity and *slope* was the slope of linearly rising phase of each input. The slope of each input varied from trial to trial from a different normal distribution with a certain mean, μ, and standard deviation, σ for each input. The value of the theoretical maximum SC neuronal activity of the FEF input was assumed to be larger from the theoretical maximum SC neuronal activity of the LIP input. This assumption reflected the instruction given to each subject in the beginning of each trial that they should always make the correct antisaccade even if their first eye movement was an error prosaccade.

In the model, decisions were formed via stochastic accumulating processes and contrast enhancement of the two decision signals. More specifically, the two cortically independent and spatially separated decision signals representing the reactive

(LIP) and planned (FEF) saccade signals, whose linearly rising phases were derived from two normal distributions with different means and standard deviations were integrated at opposite SC buildup cell populations, where they competed against each other via lateral excitation and remote inhibition. An ocular movement was initiated when the neuronal activities of the buildup cells reached a preset criterion level. The crossing of the preset criterion level in turn released the "brake" from the SC burst neurons and allowed them to discharge resulting in the initiation of an ocular movement.

To simulate the median reaction times, the shapes of the RT distributions of the correct antisaccades and the error prosaccades as well as the error rates of all 2075 subjects, we run the model for 1500 trials. In each trial, the slope of the reactive input took values for a normal distribution with mean μ_1 and standard deviation σ_1, whereas the slope of the planned input took values from another normal distribution with mean μ_2 and standard deviation σ_2. The mean values were estimated via a trial-and-error process, whereas the standard deviation values σ_1 and σ_2 were approximated so that the produced correct antisaccade and error prosaccade reaction times were greater than 80ms and less than 600ms. The threshold was adjusted so that the simulated error rate closely matched the observed one. Saccade reaction time (SRT) was estimated as the time taken from the first appearance of the peripheral stimulus till the time the burst activity started to deviate from zero. An additional 20ms efferent delay was also added.

To compare the SRT distributions of the experimental data with the simulated ones, we performed cluster analysis. The median RT and the inter-quartile range for antisaccades and error prosaccades of all 2075 conscripts were grouped into ten groups. The purpose of the cluster analysis was to partition the observations into groups ("clusters") so that the pairwise dissimilarities between those assigned to the same cluster tend to be smaller than those in a different cluster. We arbitrary chose ten clusters because we wanted each cluster to have a sufficiently large number of individuals (ranging from 30 individuals to 240 individuals in each cluster). We then normalized the SRT distribution of each subject data and then added the normalized distributions for all subjects belonging to the same group. For each category we calculated its percentage relative frequency of response times. More specifically, the time interval between 80 and 600ms was divided into twenty-six categories, each lasting 20ms. For each time bin, we added the SRTs. Plots of the simulated and experimental correct antisaccade and error prosaccade % density distributions of response times for all ten groups are displayed in Figs. 3 and 4.

The mean frequency for all subjects in a group was then calculated. The discrepancy in each category between the simulated and experimental correct and error distributions was measured by the squared difference between the observed (simulated) and the expected (experimental) frequencies divided by the expected frequency ((Observed-Expected)^2/Expected). The χ^2 value was the sum of these quantities for all categories. The rejection region was set at $\chi^2 \geq \chi^2{}_{0.05}$. The χ^2 test of homogeneity showed a significant difference in two of the ten comparisons for antisaccade RT distributions and two of the ten comparisons for the error prosaccade RT distributions (see Fig. 5).

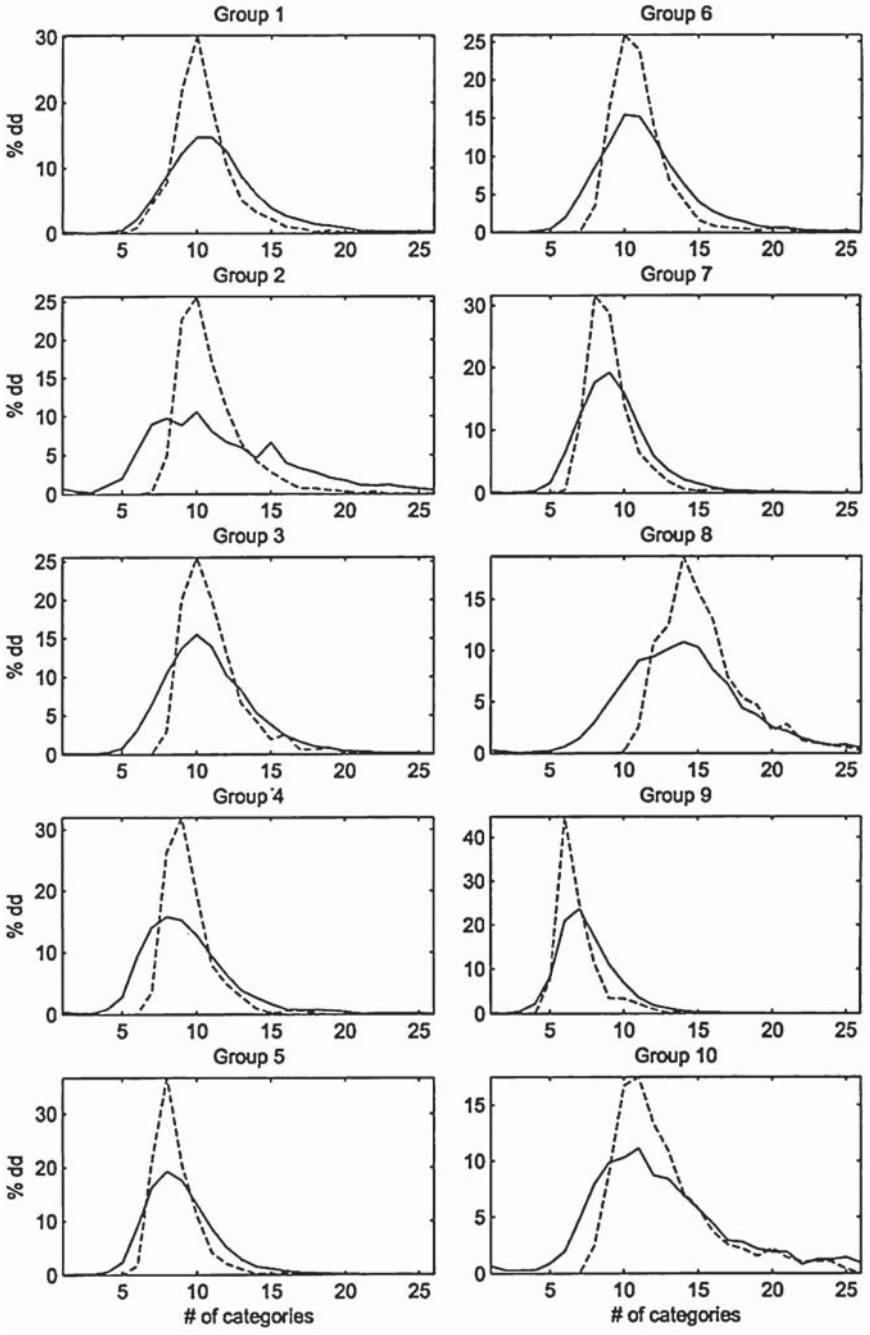

Fig. 3 Plots of correct percentage density distribution (y-axis) vs number of categories (x-axis) for all ten virtual subjects. Dashed lines: simulated correct percentage density distribution plots for all ten virtual subjects. Solid lines: experimental correct percentage density distribution plots for all ten virtual subjects. Reproduced with permission from [2], Fig. 5, p. 698, Copyright © Elsevier

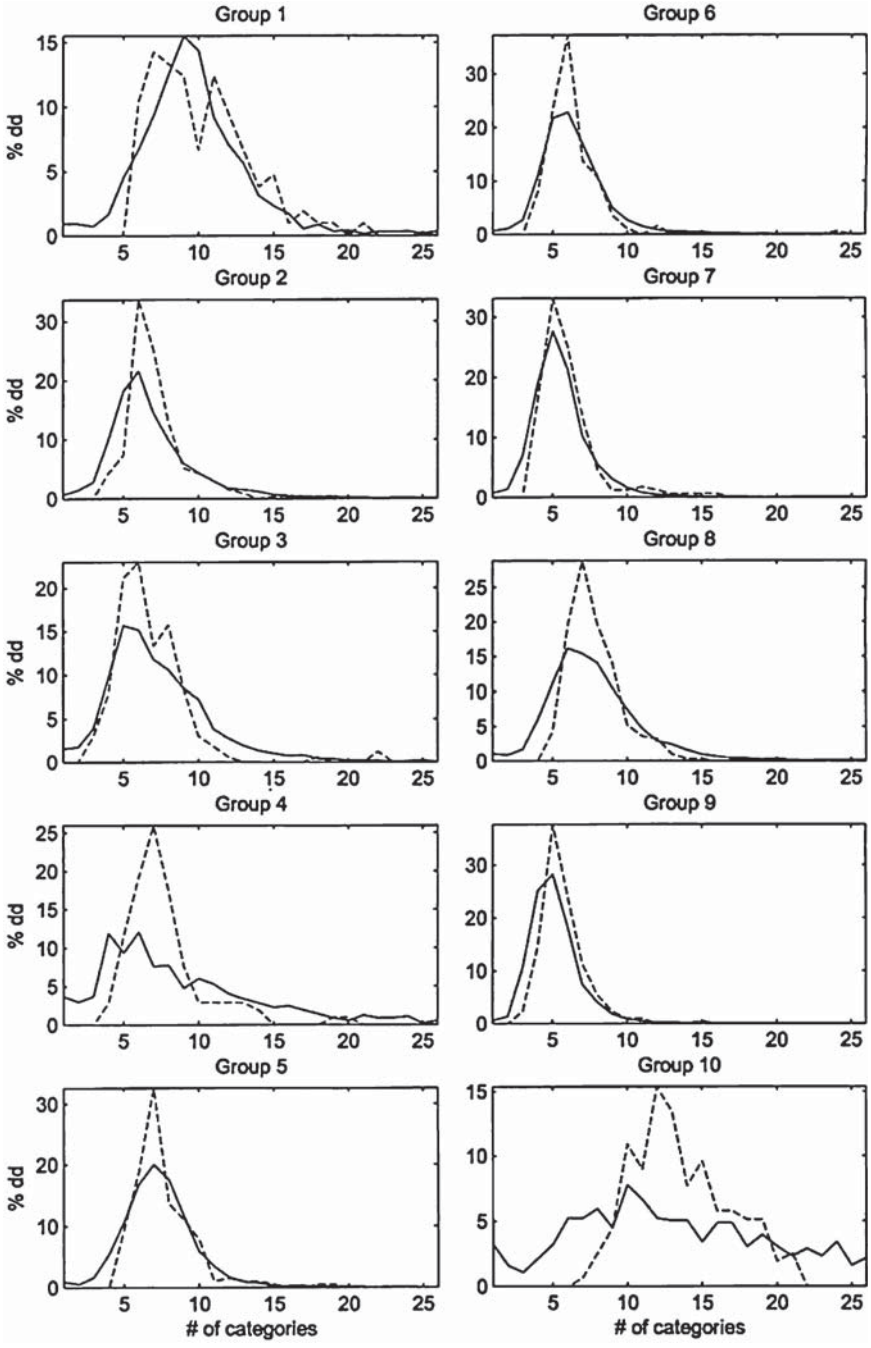

Fig. 4 Plots of error percentage density distribution (y-axis) vs number of categories (x-axis) for all ten virtual subjects. Dashed lines: simulated error percentage density distribution plots for all ten virtual subjects. Solid lines: experimental error percentage density distribution plots for all ten virtual subjects. Reproduced with permission from [2], Fig. 6, p. 699, Copyright © Elsevier

	Median correct antisaccade RT	Median error prosaccade RT	Percent antisaccade error rate	χ^2 correct antisaccades	χ^2 error prosaccades
Group 1	294.174 (288.16)	279.541 (265.20)	13.04 (16.15)	36.15	34.92
Group 2	276.50 (279.21)	202.97 (201.96)	38.62 (39.07)	90.5*	33.56
Group 3	281.89 (280.91)	212.54 (201.92)	20.15 (23.73)	32.16	32.89
Group 4	251.30 (249.27)	209.90 (211.65)	12.41 (12.02)	56.06*	96.24*
Group 5	254.80 (242.40)	212.99 (216.66)	24.27 (17.02)	35.21	24.18
Group 6	282.38 (288.44)	188.19 (193.66)	23.93 (28.86)	31.82	27.97
Group 7	263.10 (251.79)	180.63 (175.53)	20.87 (24.79)	30.34	21.82
Group 8	365.69 (349.42)	218.99 (221.36)	37.00 (34.58)	36.46	35.67
Group 9	218.20 (213.58)	177.85 (172.77)	27.36 (24.92)	36.99	23.15
Group 10	327.56 (307.5)	331.07 (326.99)	20.05 (21.81)	33.88	83.57*

Fig. 5 Simulated correct median, error median, error rate and values of χ^2 test of homogeneity between correct and error experimental and simulated percent density distributions for correct antisaccades and error prosaccades. χ^2 values marked with an asterisk indicate a significant difference between the simulated and the observed RT distributions. *Rejection region*: $\chi^2 \geq \chi^2_{0.05}$ (37.65). The degrees of freedom were 25. Units: correct SRT (ms); error SRT (ms). Values in parentheses stand for experimental values

The model was successful at explaining why the response times in the antisaccade task are so long and variable and at predicting accurately the shapes of correct and error RT distributions as well as the response probabilities of a large 2006 sample of subjects. The wealth of simulated results made the model unique in comparison to other models. The model predicted that there is no need of a top down inhibitory signal that prevented the error prosaccade from being expressed, thus allowing the correct antisaccade to be released. This finding challenged the currently accepted view of saccade generation in the antisaccade task, which requires a top-down inhibitory signal to suppress the erroneous saccade after the correct saccade has been expressed [14].

These results raised some additional important questions: (1) What are the biophysical mechanisms that produced the slowly varying climbing activity of the decision signals? (2) What are the biophysical mechanisms that produced the small varying threshold level (450 ± 50 Hz) across virtual subjects?

These questions were addressed successfully by the biophysical accumulator model summarized in the next section.

5 A Biophysical Accumulator Model

The second model [3–5], which I will call *biophysical accumulator model*, extended the previous neural SC population model of the antisaccade task by addressing the question of what were the biophysical mechanisms underlying the generation of the slowly varying accumulator like activity of the decision signals. The biophysical accumulator model was a multi-modular neural network model consisting of two cortical modules, each representing the population activity of FEF and LIP cortical

neurons that drove the SC population rate model to produce saccade reaction times (SRT) and response probabilities in the antisaccade task.

The neuronal firing rates of both cortical modules were derived from the interplay of a wealth of ionic and synaptic currents. Hodgkin-Huxley mathematical formulations were employed to model these currents and the current balance equations of pyramidal neurons and inhibitory interneurons in the networks. The current balance equation of each pyramidal neuron was given by

$$C_p \frac{dV_p}{dt} = -I_L - I_{Na} - I_{Kd} - I_{HVA} - I_{NaP} - I_C - I_{Ks} - I_{AHP} - I_{AMPA} - I_{NMDA} - I_{GABAA} + I_{inj}, \tag{5}$$

whereas the current balance equation of each inhibitory interneuron was

$$C_{inh} \frac{dV_{inh}}{dt} = -I_L - I_{Na} - I_{Kd} - I_{AMPA} - I_{NMDA} - I_{GABAA} + I_{inj}, \tag{6}$$

Each ionic current followed the general ohmic relationship

$$I_{ionic} = g_{ionic} \cdot x \cdot (V - E_{ionic}), \tag{7}$$

where g_{ionic} was the maximal conductance of the particular ion channel, and E_{ionic} was the ionic reversal potential given by the Nernst equation for the particular ionic species. x was an activation or an inactivation variable (or a combination of variables depending on the particular current being modelled, and which can be raised to a non-unity power for a better fit to the data) that determined the fraction of open channels at a given time. These variables followed first-order kinetics:

$$\frac{dx}{dt} = \alpha_x \cdot (1 - x) - \beta_x \cdot x, \tag{8}$$

where α_x and β_x were voltage-dependent rate constants. Using a voltage-dependent time constant, τ_x, and a steady-state value, x_-, the differential equation was rewritten as

$$\frac{dx}{dt} = \frac{x_\infty - x}{\tau_x}, \tag{9}$$

where

$$\tau_x = \frac{1}{\alpha_x + \beta_x} \text{ and } \quad x_\infty = \frac{\alpha_x}{\alpha_x + \beta_x}, \tag{10}$$

These types of equations were used to describe a variety of different voltage-gated ion channels. Experimentally, the steady-state activation variable could be measured using the voltage clamp protocol and fit to a Boltzmann function

$$x_\infty = \frac{1}{1 + \exp(-(V - V_{1/2})/k)}, \tag{11}$$

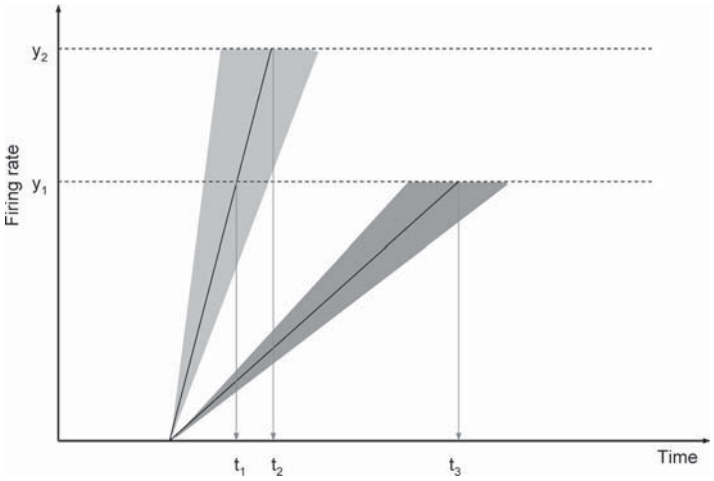

Fig. 6 Schematic diagram of the firing rate vs. time. Horizontal dashed lines depict two different threshold levels. Small increases in threshold level ($y_2 > y_1$) can result in large increases in the mean and standard deviation. Shaded area depict the variability (standard deviation) in response times

Complete mathematical formalism of the model and its parameters can be found in [3]. Both symmetric and asymmetric types of neuronal connectivities as well as homogeneous and heterogeneous neuronal firings were tested.

Detailed parametric analysis of all ionic and synaptic conductances in the model was performed to estimate which current(s) and what range of values could reproduce the full range of slope values (see Table 4 in [3]) of the planned and reactive inputs of the SC population rate model [2], while keeping the preset criterion level fixed.

It is important here to emphasize the need of keeping the criterion level fixed throughout all trials (see figure 6). Assume the criterion level is held fixed at a value y_1. Then, the resulting distribution has a mean at t_1 and a variance depicted by the light gray area. If we now move the criterion level by a small amount to y_2, then the new mean of the distribution shifts to a new value t_2 and its variance becomes much larger. That means that we have moved to a new category (i.e. a new virtual subject) with different mean and std.

The model predicted that only certain ionic and synaptic currents, namely the I_{NaP}, I_{NMDA}, and I_{AMPA} currents can produce the observed variability in the climbing activities of cortical decision signals, while keeping the preset criterion level fixed. We concluded that indirectly the model predicted the range of values of these currents' conductances' values that reproduced the correct antisaccade and error prosaccade reaction time (RT) distributions as well as response probabilities of a large group of 2006 subjects.

Acknowledgments VC was supported by the EPSRC project grant EP/D04281X/1.

References

[1] P Dayan, S Dehaene, K McCabe, R Menzel, E Phelps, H Plassmann, R Ratclif, M Shadlen, W Singer. Neuronal correlates of decision making. In: Engel C, Singer W, editors. Strungmann Forum Report: Better than conscious? Decision making, the human mind, and implications for institutions. MIT Press: Cambridge, MA, USA

[2] V Cutsuridis, N Smyrnis, I Evdokimidis, S Perantonis (2007b), "A Neural Network Model of Decision Making in an Antisaccade Task by the Superior Colliculus", *Neural Networks*, 20(6): 690–704

[3] V Cutsuridis, I Kahramanoglou, N Smyrnis, I Evdokimidis, S Perantonis (2007a), "A Neural Variable Integrator Model of Decision Making in an Antisaccade Task", *Neurocomputing*, 70(7–9): 1390–1402

[4] V Cutsuridis, I Kahramanoglou, S Perantonis, I Evdokimidis, N Smyrnis, "A Biophysical Neural Model of Decision Making in an Antisaccade Task Through Variable Climbing Activity", In: Artificial Neural Networks: Biological Inspirations – ICANN '05, Lecture Notes in Computer Science, LNCS 3696 (Springer-Verlag, Berlin, 2005a) 205–210

[5] V Cutsuridis, I Kahramanoglou, N Smyrnis, I Evdokimidis, S Perantonis, "Parametric Analysis of Ionic and Synaptic Current Conductances in a Neural Accumulator Model with Variable Climbing Activity", *19th Conference of Hellenic Society for Neuroscience*, Patra, Greece, September 30 - October 2, 2005b

[6] V Cutsuridis, N Smyrnis, I Evdokimidis, I Kahramanoglou, S Perantonis, "Neural network modeling of eye movement behavior in the antisaccade task: validation by comparison with data from 2006 normal individuals", Program No. 72.13. 2003 Abstract Viewer/Itinerary Planner. Washington, DC: Society for Neuroscience, 2003b

[7] V Cutsuridis, I Evdokimidis, I Kahramanoglou, S Perantonis, N Smyrnis, "Neural network model of eye movement behavior in an antisaccade task", *18th Conference of Hellenic Society for Neuroscience*, Athens, Greece, October 17–19, 2003a

[8] Evdokimidis, I., Smyrnis, N., Constantinidis, T. S., Stefanis, N. C., Avramopoulos, D., Paximadis, C., et al. (2002). The antisaccade task in a sample of 2006 young men I. Normal population characteristics. Experimental Brain Research, 147, 45–52

[9] Smyrnis, N., Evdokimidis, I., Stefanis, N. C., Constantinidis, T. S., Avramopoulos, D., et al. (2002). The antisaccade task in a sample of 2006 young males II. Effects of task parameters. Experimental Brain Research, 147, 53–63

[10] Hallett, P. R. (1978). Primary and secondary saccades to goals defined by instructions. Vision Research, 18, 1279–1296

[11] von Neumann, J., & Morgenstern, O. (1944). Theory of games and economic behaviour. Princeton: Princeton Univ. Press

[12] Sutton, R. S., & Barto, A. G. (1998). Reinforcement learning: an introduction. Cambridge: MIT Press

[13] Wurtz, R. H., & Goldberg, M. E. (1989). The neurobiology of saccadic eye movements. Amsterdam: Elsevier

[14] Munoz, D. P. & Everling, S. (2004). Look away: the antisaccade task and the voluntary control of eye movement. Nat Neurosci, 5, 218–228

[15] Guitton, D., Buchtel, H. A., Douglas, R. M. (1985). Frontal lobe lesions in man cause difficulties in suppressing reflexive glances and in generating goal-directed saccades. Exp Brain Res, 58, 455–472